Meandering Spiral Waves in the 1,4-Cyclohexanedione Belousov−Zhabotinsky System Catalyzed by $Fe[batho(SO_3)_2]_3^{4-/3-}$

Niklas Manz, Brent T. Ginn, and Oliver Steinbock*

Department of Chemistry and Biochemistry, Florida State University, Tallahassee, Florida 32306-4390

Received: July 11, 2003; In Final Form: October 17, 2003

Meandering spiral waves are observed in the 1,4-cyclohexanedione Belousov−Zhabotinsky (CHD-BZ) reaction at very low concentrations (3−35 mM) of the organic substrate. The spiral tips describe hypocycle-like trajectories indicating the presence of two main rotation periods and radii. The ratio of these periods approaches 1 for decreasing concentrations of CHD. In this limit, we find Z-shaped trajectories with approximately two lobes. The use of $Fe[batho(SO_3)_2]_3^{4-/3-}$ as the BZ catalyst gives rise to extremely long rotation periods (1000−4000 s), and the tip trajectories span large areas of up to 40 mm^2. As a result of the absence of gaseous products and the high absorption of the catalyst, this particular system is ideally suited for the investigation of spiral waves in closed, thin-layer systems, such as nonuniformly curved and micropatterned media.

Introduction

Rotating spiral waves are common spatio-temporal structures in a broad variety of nonequilibrium systems.[1−3] The first spiral waves in a chemical system were observed in the Belousov−Zhabotinsky (BZ) reaction[4,5] shortly after the discovery of propagating excitation waves in thin layers of the BZ system.[6,7] These intriguing structures are also found in the CO oxidation on platinum surfaces,[8] during the aggregation of the slime mold *Dictyostelium discoideum*,[9] and as spreading depression waves on chicken retinas.[10] One of the crucial features of spiral waves is the motion of the spiral tip. The position of the tip is typically defined as the point of highest curvature along an isoconcentration line of the pattern. The motion of this open wave end can describe a variety of qualitatively different trajectories including cycloidal curves as well as simple circles. These dynamics are referred to as meandering and rigid rotation, respectively.

The dependence of the spiral tip orbits on system parameters has been intensively studied in numerical simulations of various reaction−diffusion (RD) models.[11,12] Different meandering spiral patterns are also found in a RD model of flames.[13] Although some deviations from circular cores have been reported for yeast extracts[14] and neural tissue,[15,16] systematic experiments on noncircular tip trajectories are limited to the BZ reaction. In this system, tip trajectories can follow circles, hypocycles (outwardly pointing petals), epicycles (inwardly pointing petals), or a special kind of trochoid called prolate cycloid with lobes along a straight line.[17−19] All of the corresponding studies employed BZ systems with malonic acid as the organic substrate and either cerium ions, $Fe(phen)_3^{2+}$, or $Ru(bpy)_3^{2+}$ as the catalyst/indicator. Notice that the kinetics of the reaction between the organic substrate and the oxidized catalyst is a major factor determining the characteristics of spiral tip motion. It is, therefore, interesting to provide examples of meandering spiral waves in BZ systems that do not involve any of the above reactants.

Numerical simulations suggest that spiral tips can describe trajectories that differ significantly from simple circular or cycloidal curves. Surprisingly, the very first example for this phenomenon was found in 1948.[20] Using a simple cellular automaton model of spiral activity on cardiac muscles, based on the work of Wiener and Rosenbleuth,[21] "linear spiral cores" were observed. In this intriguing case, the wavelength (i.e., pitch) of the spiral wave pattern equals the circumference of the tip trajectory, and, hence, the linear core has a length of about half a wavelength. This behavior was later also observed in numerical simulations of a modified FitzHugh−Nagumo model.[22] Linear cores as well as their closely related Z-shaped variants are expected for very slow relaxation dynamics and long refractory periods.[23] Experimental evidence for this behavior is meager and limited to investigations of highly anisotropic heart muscles using multiple electrode mapping techniques.[15,16] However, these experiments lacked the necessary resolution to yield detailed tip trajectories.

In this article, we provide the first experimental evidence for meandering spiral waves in a BZ system that employs 1,4-cyclohexanedione (CHD) as the organic substrate. The use of $Fe[batho(SO_3)_2]_3^{4-/3-}$ as a catalyst[24,25] and high-absorbance indicator allows us to study the experimental conditions that give rise to *Z*-shaped tip trajectories. The overall characteristics of this excitable RD system are expected to allow future investigations of meandering spiral waves in experimental settings that do not tolerate the use of the classic BZ reaction.

Experimental Section

The classic organic substrate (malonic acid) of the BZ system is replaced by CHD. Notice that the reaction products of CHD do not involve any gaseous compounds and, hence, no detrimental gas bubbles are formed during the experiment.[26] Stock solutions of 2.0 M $NaBrO_3$ (Fluka) and 0.5 M CHD [$C_6H_8(=O)_2$; Aldrich] are prepared in Nanopure water (18 MΩ cm). Sulfuric acid is used as purchased (5 M H_2SO_4, Riedel-de Haën). The redox catalyst $Fe[batho(SO_3)_2]_3^{4-}$ (25 mM) is prepared by mixing a 3:1 molar ratio of 4,7-diphenyl-1,10-phenanthrolinedisulfonic acid disodium salt hydrate ($C_{24}H_{14}N_2 \cdot 2NaO_3S \cdot xH_2O$; Acros) with ferrous sulfate heptahydrate (Fluka) in 25 mM H_2SO_4. The reduced and oxidized forms of this complex have absorption maxima at 535 and 602 nm, respectively. The

* To whom correspondence should be addressed. E-mail steinbck@chem.fsu.edu; phone 850-644-4824; fax 850-644-8281.

10.1021/jp036008n CCC: $25.00
Published on Web 11/20/2003

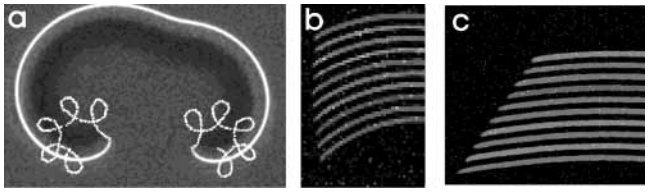

Figure 1. Noncircular tip motion of chemical waves in the CHD-BZ reaction. (a) Tip trajectories of a pair of counter-rotating spirals (white curves) superimposed onto a difference image of the wave pattern. The trajectories are obtained over a time interval of 3300 s. Field of view: 21.1 × 13.8 mm^2. (b) Superposition of 10 consecutive snapshots of a wave segment. The segment travels in an upward direction with a tangential tip velocity of approximately 0. Field of view: 7.8 × 11.3 mm^2. (c) Superposition of 10 consecutive snapshots of a shrinking wave segment with a constant but negative tangential velocity. Field of view: 11.7 × 10.8 mm^2. Frames b and c are based on difference images and illustrate the dynamics during 540 s. Initial concentrations for all three experiments: $[H_2SO_4] = 90$ mM; $[NaBrO_3] = 100$ mM; $[Fe[batho(SO_3)_2]_3^{4-}] = 0.5$ mM; and [CHD] = 30.0 mM (a), 37.5 mM (b), and 40.0 mM (c).

reduced state is dark red with a high molar absorptivity of 22 100 M^{-1} cm^{-1} at 535 nm.[25] Some experiments are carried out with $Fe(phen)_3^{2+/3+}$ (ferroin/ferriin) as the BZ redox catalyst/indicator. The ferroin sulfate solution (25 mM in 25 mM H_2SO_4) is purchased from Fluka and used without further purification. The maximal molar absorbtivity of ferroin is 11 000 M^{-1} cm^{-1} at 510 nm.

In all experiments, the concentrations of the catalyst and sulfuric acid are 0.5 and 90 mM, respectively. Notice that, after the preparation of the reaction solution, the system remains homogeneously oxidized for up to 6 h. Quasi-two-dimensional reaction conditions are created between two circular polystyrene plates with a diameter of 10 cm. The height of the resulting BZ layer is 0.39 ± 0.02 mm. The differences in the absorption spectra of the reduced solution state and the oxidized waves are monitored with a monochrome charge-coupled-device camera (COHU 2122).[27] The video signal is digitized using an image-acquisition card (Data Translation DT3155, 640 × 480 pixel, 8 bit/pixel). Image data are acquired every 2.0 s with commercial software (HLImage++97). The spiral trajectories are analyzed on a personal computer with programs written in IDL (interactive data language from Research System, Inc., version 5.1.1). All experiments are performed at 24 ± 1 °C.

Results

Earlier investigations on wave propagation in the CHD-BZ reaction focused on reaction conditions with relatively high concentrations of sulfuric acid and CHD. In these systems, spiral waves carry out rigid rotation around very small circular cores. However, at low concentrations of the aforementioned compounds, noncircular motion of open wave ends can be observed. Figure 1 shows three representative examples for qualitatively different modes of tip motion as found for $[H_2SO_4] = 90$ mM, $[NaBrO_3] = 100$ mM, and $[Fe[batho(SO_3)_2]_3^{4-}] = 0.5$ mM. Figure 1a depicts a pair of meandering spiral waves at [CHD] = 30 mM. The data are obtained by image subtraction of subsequent frames ($\Delta t = 10$ s). Hence, bright and dark areas correspond to regions of increasing and decreasing concentrations of the oxidized catalyst, respectively. Superposed are the trajectories of the counter-rotating spiral tips. In this example, the spiral tips are traced for 3300 s and, as in all subsequent analyses, their locations are determined as the points of highest local curvature at the open end of the wave front. Figure 1b,c shows the dynamics of traveling waves as observed beyond the

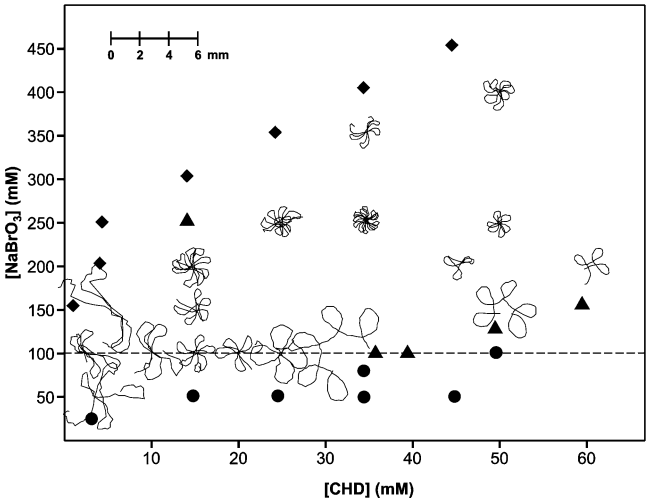

Figure 2. Tip trajectories for various concentrations of CHD and $NaBrO_3$. Diamond-shaped symbols and solid circles denote homogeneously oxidized and reduced states, respectively. Triangles denote concentrations that give rise to tip motion with nonpositive tangential velocities (cf. Figure 1b,c). The initial concentrations of H_2SO_4 and $Fe[batho(SO_3)_2]_3^{4-}$ are kept constant at 90 and 0.5 mM, respectively. The dashed line indicates a particular sodium bromate concentration (100 mM) for which many of the following individual results are taken.

stability boundary of spiral waves at elevated concentrations of CHD. At [CHD] = 37.5 mM, the tangential velocity of the open wave ends is nearly 0. Accordingly, one finds finite-length wave segments that have a characteristic convex shape (Figure 1b). Although these segments are only marginally stable, they can propagate long distances without changing their length or shape.[18] A further increase of the CHD concentrations to 40 mM results in negative tangential velocities and, hence, shrinking wave segments (Figure 1c). Notice that the behavior shown in Figure 1b,c has been also observed in the malonic acid BZ reaction.[28,29]

We emphasize that the induction times of reaction systems similar to that in Figure 1 are extremely long. During the induction time, no wave propagation is observed and the medium remains homogeneously oxidized. As mentioned previously, the induction time depends on the initial concentrations employed. In our experiments, it increases with decreasing CHD concentrations from about 3.5 h for [CHD] = 60 mM to 6 h for 3.0 mM at $[NaBrO_3] = 100$ mM. This is in qualitative agreement with the data provided in ref 30. Moreover, the induction time increases with increasing concentrations of sodium bromate ion from 4 h for $[NaBrO_3] = 50$ mM to 6 h for 250 mM at [CHD] = 15 mM.

The rotation dynamics of spiral waves are most sensitive to the concentrations of the reactants.[31] Figure 2 shows tip orbits found for various concentrations of CHD and $NaBrO_3$. The trajectories are plotted with respect to one particular length scale, which allows for simple comparison of their size. Each curve is centered at the coordinates of the corresponding reactant concentrations. The flowerlike orbits have a hypocyclic character because their lobes are pointing in the outward direction. Within the parameter space investigated, all spiral waves carry out meandering tip motion and we observe neither epicyclic trajectories nor rigid rotation around circular cores. Moreover, the phase diagram in Figure 2 reveals that spiral waves are confined to a particular stability island. At the high and low bromate fringes of this island, one detects marginally stable and shrinking wave segments similar to those shown in Figure 1b,c. The corresponding concentration pairs are denoted by solid

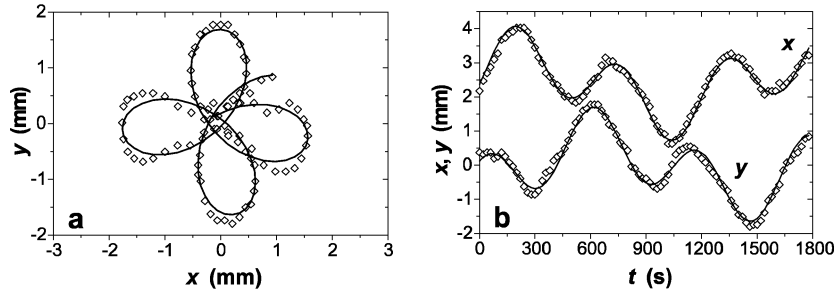

Figure 3. Comparison of the motion of a meandering spiral tip with its rms-minimized fit to a hypocycle (cf. eq 1). The experimental data (open diamonds) and the corresponding fit (straight line) are shown in the *xy* plane (a) and in terms of the temporal evolution of the *x* and *y* values (b) with *x* values being offset by 2.5 mm. The starting point of the counterclockwise motion is near the origin of the pattern. Fit parameters: $r_1 = 0.90$ mm, $r_2 = 0.78$ mm, $T_1 = 570$ s, and $T_2 = 530$ s. Initial concentrations are the same as those in Figure 1 except [CHD] = 25.0 mM.

triangles. Outside of the island of spiral and spiral-like motion, we find spatially homogeneous systems. These wave-free reaction systems remain in an either oxidized or reduced state for high and low concentrations of bromate, respectively.

Before we proceed with a closer inspection of the tip trajectories, we must introduce a more detailed description of their main features. Uniformly rotating spiral tips with a circular spiral core are characterized by a unique core radius r_1 and a constant rotation period T_1. In a meandering system, the radius r_1 becomes the average radius of the petals. The petals arise from a superimposed rotation of a second circle of radius r_2 and period T_2. To obtain hypocyclic motion, the rotation directions of these circles have to be in opposite directions. The trajectories of such a meandering spiral tip are described by

$$x = r_1 \cos(\omega_1 t + \varphi_1) - r_2 \cos(\omega_2 t + \varphi_2) + x_0$$
$$y = r_1 \sin(\omega_1 t + \varphi_1) + r_2 \sin(\omega_2 t + \varphi_2) + y_0 \qquad (1)$$

where x and y denote the Cartesian coordinates of the spiral tip, t indicates time, and φ_1 and φ_2 are constants representing the phase of spiral motion at time $t = 0$. The parameters x_0 and y_0 define the Cartesian coordinates of the center of the tip trajectory. The angular velocities ω_1 and ω_2 equal $2\pi/T_1$ and $2\pi/T_2$, respectively. We use eq 1 to extract the physically relevant quantities r_1, r_2, T_1, and T_2 from the observed motion of meandering spiral tips. Our fitting procedure minimizes the root-mean-square (rms) deviation between the experimental data and eq 1 by optimizing a total of eight parameters, namely, the values of the radii, the angular frequencies, the phase factors, and the coordinate offset. Special care is taken to choose appropriate initial values for the fitting parameters because the discrete nature of the experimental data can generate low rms results for unrealistic, high-frequency motion. Inappropriate fits, however, can be easily dismissed because they yield one period that is approximately equal to or smaller than the experimental sampling rate.

Figure 3 shows a typical example of a fit obtained using the procedure outlined previously. In Figure 3a, the data points and the fit are displayed in the *xy* plane as open diamonds and a solid line, respectively. Figure 3b illustrates the temporal evolution of the tip's Cartesian coordinates and the corresponding fit in terms of its *x* and *y* values. For clarity, the two curves in Figure 3b are separated by adding a constant offset of 2.5 mm to all *x* values. In this particular example, we obtain values of $r_1 = 0.90$ mm, $r_2 = 0.78$ mm, $T_1 = 570$ s, and $T_2 = 1530$ s. The fitting procedure yields very good agreement with the experimental data. However, it should be noted that some tip trajectories show deviations from an ideal hypocyclic shape that are not recovered by eq 1. Nonetheless, our analysis provides accurate results for the principal rotation periods and radii.

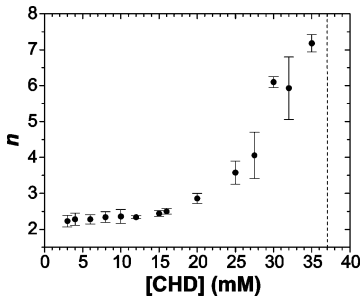

Figure 4. Dependence of the number of lobes n on the initial concentration of CHD. All other concentrations are kept constant at the values given in Figure 1. The dashed line at [CHD] = 37 mM indicates the boundary of stable wave fronts.

Another important parameter of meandering spirals is the number of petals, n, of the tip trajectory. For meandering waves that give rise to hypocyclic trajectories, n can be calculated as

$$n = \omega_1/\omega_2 + 1 = T_2/T_1 + 1 \qquad (2)$$

For the example shown in Figure 3, we find $n = 3.6 \pm 0.3$. Notice that the quantity n is typically not an integer value and the tip trajectory, therefore, closes itself only after a large or infinitely large number of rotations. Moreover, quantitative analysis of the data in Figure 2 reveals a decrease in the number of petals as the concentration of bromate ion is increased. In addition, the main rotation periods and the overall size of the tip trajectories decrease with increasing concentrations of bromate ion. Changing the sulfuric acid concentration to values higher than 90 mM decreases the rotation periods involved but has no influence on the number of petals. A decrease of the acidity, however, leads to longer rotation periods and increasing values of n. For example, at [CHD] = 50 mM and [$NaBrO_3$] = 250 mM, we find that n increases from 2.7 ± 0.1 to 5.2 ± 0.2 as the concentration of sulfuric acid is lowered from 90 to 50 mM. This change in the number of petals results from a disproportional increase of the rotation periods of the orbiting circle (T_1) and the orbited circle (T_2). For the given concentrations, no wave propagation is observed above 400 mM and below 40 mM sulfuric acid, and the system remains homogeneously oxidized or reduced, respectively.

Figure 4 shows the dependence of n on the initial concentration of CHD. The concentrations of H_2SO_4, $NaBrO_3$, and $Fe[batho(SO_3)_2]_3^{4-}$ are kept constant at 90, 100, and 0.5 mM, respectively. Under these conditions, spirals are stable up to a maximal CHD concentration of 35 mM. At higher concentrations, one observes wave segments with negative tangential velocities or homogeneously reduced media. The data shown in Figure 4 reveal that the number of lobes, n, decreases with decreasing concentrations of the organic substrate and saturates

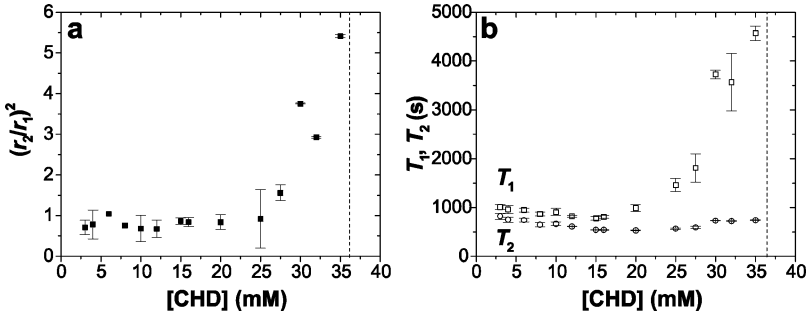

Figure 5. Dependence of the squared ratio of the radii r_2 and r_1 (a) and the rotation periods T_1 and T_2 (b) on the initial concentration of CHD. All other concentrations are kept constant at the values given in Figure 1. The dashed line indicates the boundary of stable wave fronts.

to a value of $n \approx 2$ in the limit of small concentrations. Neither rigid rotation nor epicyclic trajectories are observed.

Figure 5 complements the information of Figure 4 by providing data on the concentration-dependent changes of the radii ratio and the rotation periods. As shown in Figure 5a, the ratio $(r_2/r_1)^2$ remains constant at a value slightly smaller than 1.0 for CHD concentrations below 25 mM. Between 25 and 35 mM, this quantity increases steadily to about 5.5. Above [CHD] $\approx$ 35 mM, no spiral waves exist. The rotation period T_1 shows a similar dependence as the radii ratio, whereas T_2 remains essentially constant over the entire concentration range (Figure 5b). Notice that the inequality $T_1 > T_2$ is characteristic for hypocycles. Moreover, the transition from $r_2/r_1 < 1$ to $r_2/r_1 > 1$ marks a qualitative change in the shape of the tip trajectory. For ratios much greater than unity, the lobes of the trajectories are separated by long arches. At $r_2/r_1 = 1$, the lobes touch each other at the pattern's central point and overlap for smaller ratios.

The data in Figure 5 can be used to discuss the absence of small circular cores and epicycles in our experiments. According to theoretical analyses, the onset of meandering is a supercritical Hopf bifurcation.[12,32] In this case, the squared radii ratio of the orbited and orbiting circle $(r_2/r_1)^2$ should increase linearly with the distance of the control parameter from the transition point. At the Hopf bifurcation, the ratio must be 0 because the orbited circle of radius r_2 disappears. The spiral tip dynamics in the CHD-BZ system for [CHD] = 25−35 mM is in qualitative agreement with these expectations (cf. Figure 5). At lower concentration values, however, the ratio is constant and does not further decrease to $(r_2/r_1)^2 = 0$. Therefore, the transition to circular cores is not observed, but a transition toward a different type of tip orbit that we describe in the following takes place.

The low-concentration limit of the data in Figures 4 and 5 corresponds to a remarkable tip trajectory that has attracted much attention in the literature. Below [CHD] $\approx$ 5.0 mM, the typical flowerlike tip trajectory approaches an elongated Z-shaped orbit. A representative example of this unusual phenomenon is shown in Figure 6. This type of spiral core was first found by Fast et al. in a modified cellular automaton model[23] but had not been observed yet in a chemical RD system. The Z-shaped trajectory represents a transition state between cycloidal trajectories and linear cores. Notice that, for Z-shaped as well as linear orbits, the rotation period and the refractory phase of the system are of similar duration. Similar results were also obtained in numerical simulations of a modified FitzHugh−Nagumo model[22] and the Beeler−Reuter model of cardiac tissue.[33]

The occurrence of Z-shaped tip trajectories in our experiments coincides with a dramatic increase of the pattern wavelength, which seems to be in good agreement with the theoretical predictions. For example, the wavelength of the spiral wave in Figure 6 is approximately 16 mm, thus, indicating a remarkably long refractory phase or high excitation threshold. Moreover,

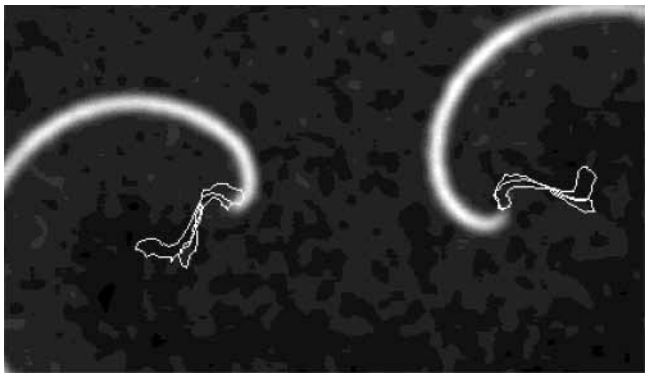

Figure 6. Z-shaped tip trajectories of a counter-rotating spiral pair as observed during 1800 s. The trajectories (white curves) are superposed onto a snapshot of the wave pair, which is obtained by image subtraction of consecutive video frames (Δt = 40 s). Initial concentrations: [H_2SO_4] = 90 mM, [CHD] = 3.0 mM, [$NaBrO_3$] = 100 mM, and [$Fe[batho(SO_3)_2]_3^{4-}$] = 0.5 mM. Field of view: 32.4 × 19.7 mm^2.

the circumference of the Z-shaped tip trajectory is approximately 7.5 mm and, hence, about half a wavelength as expected for near-linear orbits. We also attempted to find Z-shaped trajectories in the ferroin-catalyzed CHD-BZ reaction. Although the latter system shows meandering spiral waves within the concentration ranges investigated here, no wave propagation could be detected at the low CHD concentrations that give rise to Z-shaped orbits in the $Fe[batho(SO_3)_2]_3^{4-}$-catalyzed reaction. This seeming absence of spiral waves could be due to insufficient sensitivity of the detection equipment because absorption changes are less pronounced in the ferroin-catalyzed reaction. On the other hand, the Z-shaped orbits shown in Figure 6 might be the result of the slower relaxation kinetics in the $Fe[batho(SO_3)_2]_3^{4-}$ system that gives rise to significantly larger wavelengths.

Conclusions

In this study, we provide the first example of meandering spiral waves in a RD system other than the malonic acid BZ reaction. The rotation period and wavelength of the rotating wave patterns are surprisingly long as the result of slow relaxation kinetics between $Fe[batho(SO_3)_2]_3^{4-}$ and CHD as well as CHD-derived organic intermediates. The use of this particular, high-absorbance redox catalyst/indicator also assists in the optical detection of chemical waves at low concentrations of reactants. These features allow us to investigate extreme concentration ranges in which we observe Z-shaped tip trajectories.

Our experiments show that the period ratio T_2/T_1 of meandering spirals increases with increasing concentrations of CHD and decreasing concentrations of H_2SO_4 and $NaBrO_3$. This finding is qualitatively similar to the behavior of the malonic acid BZ

reaction. In the CHD-BZ reaction, however, the concentration range for meandering spirals is shifted to lower concentrations of the organic substrate. Moreover, in the concentration range investigated, the reaction shows neither rigid rotation nor epicyclic tip trajectories. Instead, we observe continuous progressions of hypocyclic orbits. These findings, however, do not rule out the possibility that epicyclic patterns may exist in the CHD-BZ reaction within a very narrow window of parameter values or for significantly different sets of reactant concentrations.

Another difference between these two reaction systems relates to the velocity−wavelength dependence of chemical wave trains. The dispersion relation in the classic BZ reaction is monotonically increasing, whereas the CHD-BZ system shows anomalous dispersion over a wide range of reactant concentrations.[34,35] For the parameter space investigated here, we could not find any evidence for anomalous dispersion. However, it is possible that in the CHD-BZ reaction meandering tip motion exists under conditions that show nonmonotonic dispersion relations. As a result of the lack of theoretical analyses in the literature, it is difficult to discuss how such a scenario would influence the dynamics of spiral tips. Obviously, more work is needed to clarify this interesting question.

The study of unperturbed and externally forced spiral tip dynamics continues to attract considerable attention. Current research focuses on the study of spiral wave drift under feedback-controlled forcing,[36,37] meandering-like instabilities of rotating three-dimensional structures,[38] and wave propagation in heterogeneous[39,40] and micropatterned media.[25,41] The high absorbance characteristics, the lack of gaseous products, and the presence of meandering spiral waves make the Fe[batho-$(SO_3)_2]_3^{4-}$-catalyzed CHD-BZ reaction an ideally suited system for the systematic investigation of all of these topics.

Acknowledgment. This work was supported by the National Science Foundation (NSF Grant CHE-20023105). N.M. thanks the "Deutsche Akademie für Naturforscher Leopoldina" (Grant BMBF-LPD 9901/8-85) for financial support.

References and Notes

(1) Field, R. J., Burger, M., Eds. *Oscillations and Traveling Waves in Chemical Systems*; Wiley: New York, 1985.
(2) Holden, A. V., Markus, M., Othmer, H. G., Eds. *Nonlinear Wave Processes in Excitable Media*; Plenum: New York, 1991.
(3) Epstein, I. R.; Pojman, J. A. *An Introduction to Nonlinear Chemical Dynamics*; Oxford University Press: New York, 1998.
(4) Winfree, A. T. *Science* **1972**, *175*, 634.
(5) Zhabotinsky, A. M.; Zaikin, A. N. *J. Theor. Biol.* **1973**, *40*, 45.
(6) Belousov, B. P. In *Oscillations and Traveling Waves in Chemical Systems*; Field, R. J., Burger, M., Eds.; Wiley: New York, 1985; p 605.
(7) Zaikin, A. N.; Zhabotinsky, A. M. *Nature* **1970**, *225*, 535.
(8) Jakubith, S.; Rotermund, H. H.; Engel, W.; von Oertzen, A.; Ertl, G. *Phys. Rev. Lett.* **1990**, *65*, 3013.
(9) Gerisch, G. *Naturwissenschaften* **1971**, *58*, 430.
(10) Gorelova, N. A.; Bureš, J. *J. Neurobiol.* **1983**, *14*, 353.
(11) Zykov, V. S. *Simulation of Wave Processes in Excitable Media*; Manchester University Press: New York, 1987.
(12) Barkley, D. In *Chemical Waves and Patterns*; Kapral R., Showalter, K., Eds.; Kluwer Academic: Dordrecht, The Netherlands, 1995; p 163.
(13) Panfilov, V.; Bayliss, A.; Matkowsky, B. J. *Appl. Math. Lett.* **2003**, *16*, 131.
(14) Mair, T.; Müller, S. C. *J. Biol. Chem.* **1996**, *271*, 627.
(15) Dillon, S.; Ursell, P. S.; Wit, A. L. *Circulation* **1985**, *72* (Suppl. III), 1116.
(16) Frazier, D. W.; Wolf, P. D.; Wharton, J. M.; Tang, A. S. L.; Smith, W. M.; Ideker, R. E. *J. Clin. Invest.* **1989**, *83*, 1039.
(17) Müller, S. C.; Plesser, Th.; Hess, B. *Physica D* **1987**, *24*, 87.
(18) Nagy-Ungvarai, Zs.; Ungvarai, J.; Müller, S. C. *Chaos* **1993**, *3*, 15.
(19) Guo, H.; Li, L.; Ouyang, Q.; Liu, J.; She, Z. *J. Chem. Phys.* **2003**, *118*, 5038.
(20) Selfridge, O. *Arch. Inst. Cardiol. Mex.* **1948**, *18*, 177.
(21) Wiener, N.; Rosenblueth, A. *Arch. Inst. Cardiol. Mex.* **1946**, *16*, 205.
(22) Krinsky, V. I.; Efimov, I. R.; Jalife, J. *Proc. R. Soc. London, Ser. A* **1992**, *437*, 645.
(23) Fast, V. G.; Efimov, I. R.; Krinsky, V. I. *Phys. Lett. A* **1990**, *151*, 157.
(24) Yamaguchi, T.; Kuhnert, L.; Nagy-Ungvarai, Zs.; Müller, S. C.; Hess, B. *J. Phys. Chem.* **1991**, *95*, 5831.
(25) Ginn, B. T.; Steinbock, B.; Kahveci, M.; Steinbock, O. *J. Phys. Chem. A*, submitted for publication.
(26) Kurin-Csörgei, K.; Szalai, I.; Molnár-Perl, I.; Körös, E. *React. Kinet. Catal. Lett.* **1994**, *53*, 115.
(27) Müller, S. C.; Plesser, Th.; Hess, B. *Physica D* **1987**, *24*, 71.
(28) Nagy-Ungvarai, Z.; Pertsov, A. M.; Hess, B.; Müller, S. C. *Physica D* **1992**, *61*, 205.
(29) Nagy-Ungvarai, Z.; Müller, S. C. *Int. J. Bifuration & Chaos* **1994**, *4*, 1257.
(30) Kurin-Csörgei, K.; Zhabotinsky, A. M.; Orbán, M.; Epstein, I. R. *J. Phys. Chem.* **1996**, *100*, 5393.
(31) Belmonte, A. L.; Ouyang, Q.; Flesselles, J.-M. *J. Phys. II (France)* **1997**, *7*, 1425.
(32) Barkley, D. *Phys. Rev. Lett.* **1994**, *72*, 164.
(33) Efimov, I. R.; Krinsky, V. I.; Jalife, J. *Chaos, Solitons & Fractals* **1995**, *5*, 513.
(34) Manz, N.; Müller, S. C.; Steinbock, O. *J. Phys. Chem. A* **2000**, *104*, 5895.
(35) Hamik, C. T.; Manz, N.; Steinbock, O. *J. Phys. Chem. A* **2001**, *105*, 6144.
(36) Kheowan, O.-U.; Zykov, V. S.; Müller, S. C. *Phys. Chem. Chem. Phys.* **2002**, *4*, 1334.
(37) Sakurai, T.; Mihaliuk, E.; Chirila, F.; Showalter, K. *Science* **2002**, *296*, 2009.
(38) Qu, Z.; Xie, F.; Garfinkel, A. *Phys. Rev. Lett.* **1999**, *83*, 2668.
(39) Bub, G.; Shrier, A. *Chaos* **2002**, *12*, 747.
(40) Davydov, V. A.; Manz, N.; Steinbock, O.; Zykov, V. S.; Müller, S. C. *Phys. Rev. Lett.* **2000**, *85*, 868.
(41) Suzuki, K.; Yoshinobu, T.; Iwasaki, H. *J. Phys. Chem. A* **2000**, *104*, 6602.